^{17}O NMR Study of Water Exchange on $[Gd(DTPA)(H_2O)]^{2-}$ and $[Gd(DOTA)(H_2O)]^{-}$ Related to NMR Imaging[1,2]

Károly Micskei,[†,‡] Lothar Helm,[†] Ernö Brücher,*[,‡] and André E. Merbach*[,†]

Institut de Chimie Minérale et Analytique, Place du Château 3, CH-1005 Lausanne, Switzerland, and Institute of Inorganic and Analytical Chemistry, Kossuth University, H-4010 Debrecen, Hungary

Received April 6, 1993

The water-exchange rate constants for the $[Gd(DTPA)(H_2O)]^{2-}$ and $[Gd(DOTA)(H_2O)]^{-}$ complexes as determined by variable-temperature ^{17}O NMR are respectively $k_{ex}^{298} = (4.1 \pm 0.3) \times 10^6$ and $(4.8 \pm 0.4) \times 10^6$ s^{-1}. The activation volumes ($\Delta V^{\ddagger}$), measured up to 200 MPa, are 12.5 ± 0.2 and 10.5 ± 0.2 cm^3 mol^{-1}, indicating an extreme dissociative activation mode for the water-exchange mechanism. The mechanism (D) is further supported by the large activation enthalpies ($\Delta H^{\ddagger} = +52.0 \pm 1.4$ and $+48.8 \pm 1.6$ kJ mol^{-1}) and positive entropies ($\Delta S^{\ddagger} = +56.2 \pm 5$ and $+46.6 \pm 6$ kJ mol^{-1} K^{-1}) obtained for the $[Gd(DTPA)(H_2O)]^{2-}$ and $[Gd(DOTA)(H_2O)]^{-}$ complexes, respectively. In the first coordination sphere of these two monoaqua complexes there is only space for one water molecule, and thus the bond breaking of the coordinated water should be the rate-determining step. The ^{17}O relaxation contribution of the second coordination sphere was estimated by investigating $[Gd(TETA)]^{-}$, which has no water in the first coordination sphere. All these considerations lead to the conclusion that the effectiveness of $[Gd(DTPA)(H_2O)]^{2-}$ and $[Gd(DOTA)(H_2O)]^{-}$ as contrast agents in MRI is not limited by the relatively low water-exchange rates but by T_{1m}, the longitudinal relaxation time of water protons in the first coordination sphere.

Introduction

In recent years magnetic resonance imaging (MRI) became an important clinical modality in diagnostic medicine.[3] The MRI signal mainly comes from the protons of the water molecules in the body fluids and tissues. The signal intensities, and therefore the image contrast, depend on the longitudinal ($1/T_1$) and transverse ($1/T_2$) relaxation rates of the water protons. It is common to increase the contrast of the images by increasing the relaxation rates by addition of paramagnetic substances, so-called MRI contrast agents. An acceleration of relaxation can be achieved by adding paramagnetic ions like Gd^{3+}, Fe^{3+}, and Mn^{2+}, which are in an electron spin S ground state at the oxidation states indicated. Unfortunately these ions are very toxic in a free state when they are injected into the body in concentrations necessary for their use as relaxation agents. Therefore only very stable and inert complexes of these ions are employed. Besides the strong complexation, the ligands used have to allow water molecules to enter into the first coordination sphere of the metal ion and by rapid exchange with water in the outer coordination shell ensure the desired effect of relaxation enhancement.

The most widely used contrast agents nowadays are complexes of gadolinium(III) such as $[Gd(DTPA)(H_2O)]^{2-}$ and $[Gd(DOTA)(H_2O)]^{-}$ (for the structures of the ligands see Figure 1).[4-6] These complexes are extremely inert and contain one water molecule in the first coordination shell, according to X-ray diffraction data on $[Gd(DTPA)(H_2O)]^{2-}$,[7] $[Nd(DTPA)(H_2O)]^{2-}$,[8] and $[Eu(DOTA)(H_2O)]^{-}$ [9] and ^1H and ^{13}C NMR as well as luminescence studies on $[Ln(DTPA)(H_2O)]^{2-}$ and $[Ln(DOTA)(H_2O)]^{-}$.[10-12] These studies also show that all donor atoms of DTPA and DOTA are actually coordinated to the ion. Similar studies using the TETA ligand[12,13] (see Figure 1 for structure) show that in this case no water molecules enter into

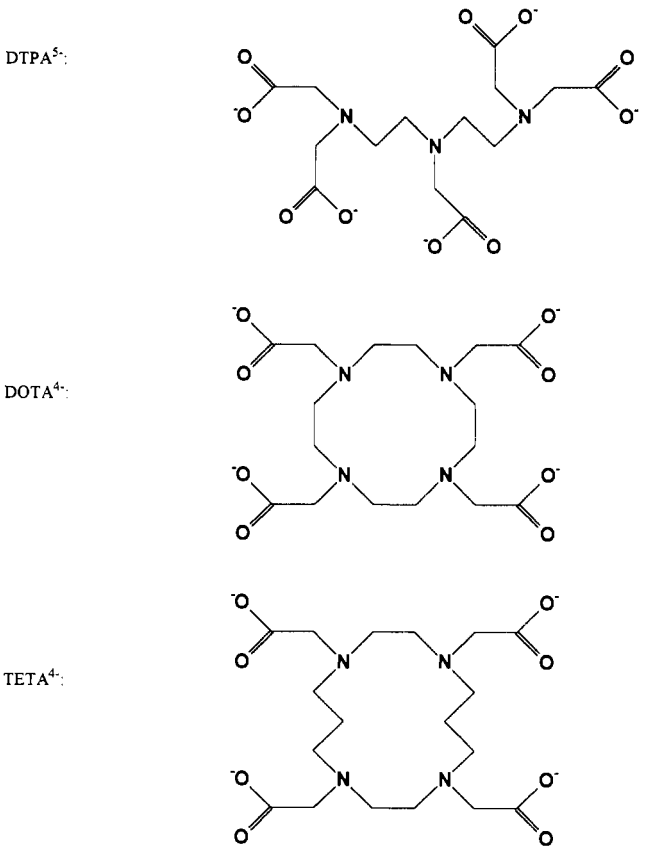

Figure 1. Schematic drawing of the ligands used in this study ($DTPA^{5-}$ = diethylenetriamine-*N,N',N'',N'''*-pentaacetate; $DOTA^{4-}$ = 1,4,7,10-tetraazacyclododecane-*N,N',N'',N'''*-tetraacetate; $TETA^{4-}$ = 1,4,8,11-tetraazacyclotetradecane-*N,N',N'',N'''*-tetraacetate).

† Institut de Chimie Minérale et Analytique.
‡ Kossuth University.

(1) High-Pressure NMR Kinetics. 58. For part 57, see ref 2.
(2) Abou-Hamdan, A.; Burki, N.; Lincoln, S. F.; Merbach, A. E.; Vincent, S. *Inorg. Chim. Acta* **1993**, *207*, 27.
(3) Bünzli, J.-C. G.; Choppin, G. R. *Lanthanide Probes in Life, Chemical and Earth Sciences*; Elsevier: Amsterdam, 1989; Chapter 5.
(4) Lauffer, R. B. *Chem. Rev.* **1987**, *87*, 901.
(5) Goldstein, H.; Lumma, W.; Rudzik, A. *Annu. Rep. Med. Chem.* **1989**, *24*, 265.
(6) Desreux, J. F.; Barthelemy, P. P. *Nucl. Med. Biol.* **1988**, *15*, 9.
(7) Gries, H.; Miklautz, H. *Physiol. Chem. Phys. Med. NMR* **1984**, *16*, 105.
(8) Stezowski, J. J.; Hoard, J. L. *Isr. J. Chem.* **1984**, *24*, 323.
(9) Spirlet, M. R.; Rebizant, J.; Desreux J. F.; Loncin, F. *Inorg. Chem.* **1984**, *23*, 359.

0020-1669/93/1332-3844$04.00/0

the first coordination shell, making this complex much less attractive as a contrast agent.

The relaxation enhancement of water protons caused by these substances is measured by ^1H NMR and is normally interpreted using the Solomon–Bloembergen–Morgan (SBM) theory,[4] as well as the equations given by Swift and Connick.[14] One important factor in this theory is the rate constant of water exchange between the first coordination sphere of the metal ion and the outer coordination shell, which transfers the fast relaxation of a nuclear spin when coupled to an electron spin into the bulk of the water solution. To obtain a maximum effect, the residence time, τ_m, of a water molecule in the bound state, which is the reciprocal of the exchange rate constant, k_{ex}, has to be of the right order of magnitude, 10^{-6}–10^{-9} s, depending on different factors such as the electron spin relaxation rate and the molecular tumbling time of the complex.[4]

Water-exchange rates for triply charged cations in general extend over more than 18 orders of magnitude.[15] The lanthanide aqua ions are all situated at the very fast exchange side of the whole exchange rate spectrum, with rate constants in the range 10^7–10^9 s^{-1}.[16] Until now, very little information is available on water exchange rates of cations with multidentate ligands used as contrast agents. Southwood-Jones et al. published[17] exchange rates for $[Gd(PDTA)(H_2O)_2]^-$ which are about 3 times slower than those for the neat aqua complex. This is in contrast to observations made on first-row transition metals, where coordination of anionic ligands labilizes the metal–water bond[18] and leads therefore to faster exchange rates.

The water-exchange rate, which is the exchange rate of the oxygen atom, represents a lower limit for the exchange rate of the water protons. In these fast exchanging systems it may be expected to be very close to the proton-exchange rate, and so it is important for a better understanding of the mode of operation of the relaxation agents based on these gadolinium complexes. Furthermore, it has been shown that variable-temperature and variable-pressure ^{17}O NMR can provide information on the exchange reaction mechanism. We found it worthwhile, therefore, to perform a complete ^{17}O NMR study on $DTPA^{5-}$ and $DOTA^{4-}$ complexes of Gd^{3+}. The $[Gd(TETA)]^-$ complex, having no water in the first coordination sphere, was included because it provides us for the first time with information on the possible contribution of second-coordination-sphere effects on ^{17}O relaxation on lanthanide complexes.

Experimental Section

Chemicals and Solutions. $Gd(ClO_4)_3$ and $Eu(ClO_4)_3$ stock solutions were prepared by dissolving excess Gd_2O_3 and Eu_2O_3 (NUCOR Corp., Phoenix, AZ; 99.99%) in perchloric acid (Merck, p.a., 70%). The pHs of the solutions were regulated after filtration to 4. The lanthanide concentration was determined by chelatometric titration with Na_2H_2-EDTA solution using xylenol orange as indicator and urotropin for pH regulation.

H_5DTPA was purchased from Fluka (puriss p.a., >99%) and H_4-DOTA was used as obtained from Schering (Berlin). H_4TETA was provided by Prof. J. F. Desreux (Liège). The purity of the ligands was checked using pH-metry, chelatometry, and ^1H NMR. All solutions were prepared by weight. To the adequate amount of solid ligand we added distilled water and decarbonated 1 M NaOH for stoichiometric deprotonation. We added a weighed amount of $Gd(ClO_4)_3$ or $Eu(ClO_4)_3$ to the solution and left it for a day for complete complexation. Then the pH of all solutions was adjusted using 1 M NaOH and/or $HClO_4$. For NMR measurements we evaporated the water of the samples under vacuum and added an identical weighed amount of 5.5% ^{17}O enriched water (Yeda). The pHs of these solutions were then checked again. The sample compositions are given in Table I.

Table I. Compositions of Samples Used for Variable-Temperature (Nos. 1–4) and Variable-Pressure (Nos. 5 and 6) ^{17}O NMR Studies

no.	aqueous soln[a]	molality/ mol kg^{-1}	ligand excess/%	10^4P_m	pH
1	$HClO_4$-acidified water				2.0
2	$[Gd(DTPA)(H_2O)]^{2-}$	0.0500	2.5	9.00	5.3
3	$[Gd(DOTA)(H_2O)]^-$	0.0504	2.3	9.07	5.1
4	$[Gd(TETA)]^-$	0.0484	6.1		7.7
5	$[Gd(DTPA)(H_2O)]^{2-}$	0.0495	3.5	8.92	5.1
6	$[Gd(DOTA)(H_2O)]^-$	0.0495	3.9	8.92	5.0

[a] 5.5% ^{17}O enriched water.

UV–Visible Measurements. Variable-temperature UV–visible measurements were performed (Perkin-Elmer Lambda 5 spectrometer) to check the possibility of the presence of coordination equilibria of the complexes studied. For this purpose we used the europium(III) complexes, which have very sensitive electronic absorption in the ranges 390 nm < λ < 400 nm and 578 nm < λ < 581 nm. The temperature dependence of these transitions was measured in the 5 °C < T < 85 °C range. All experimental details and results are collected in the supplementary material.

NMR Measurements. Variable-temperature ^{17}O NMR measurements were performed at two magnetic fields using Bruker AM-400 (9.4 T, 54.2 MHz) and AC-200 (4.7 T, 27.1 MHz) spectrometers. Bruker VT-1000 temperature control units were used to stabilize the temperature in the range 273–373 K. The temperature was measured before and after each measurement by substituting the sample with an NMR tube containing a platinum resistance thermometer.[19] The inversion recovery method[20] was applied to measure longitudinal relaxation rates, $1/T_1$, and the Carr–Purcell–Meiboom–Gill spin-echo technique[21] was used to obtain transverse relaxation rates, $1/T_2$.

All solutions were introduced into spherical glass containers, fitting into ordinary 10-mm NMR tubes, in order to eliminate magnetic susceptibility corrections to chemical shifts.[22] This technique also leads to a small gas volume above the solutions and reduces therefore problems due to distillation of water at the highest temperatures.

The elimination of magnetic susceptibility effects by the use of spherical cells was checked in the following way: The chemical shifts of a 1.00×10^{-2} m sample of $[Gd(H_2O)_8]^{3+}$ sitting in the spherical cell was measured at 25.0 °C relative to an acidified water external standard using first a superconducting NMR magnet (4.7 T) where the static magnetic field, B_0, is parallel to the cylindrical NMR tubes and then an electromagnet (1.4 T, 8.13 MHz, ^{17}O) where B_0 is perpendicular to the sample tube. If there were any distortion from spherical symmetry of the sample, for example due to solution entering the cylindrical part of the container, there would be a difference in the observed chemical shifts. The equations describing the corrections to observed chemical shifts for an infinite cylindrical shaped sample are given (eq 1 for superconducting magnets and eq 2 for electromagnets).

$$\delta^{\parallel}_{obs} = \delta + (4\pi/3)(\chi_{ref} - \chi_{sample}) \quad (1)$$

$$\delta^{\perp}_{obs} = \delta - (2\pi/3)(\chi_{ref} - \chi_{sample}) \quad (2)$$

The chemical shifts measured in the different magnets were self-consistent so the correction due to deviation from spherical geometry was negligible.

Variable-pressure NMR measurements were made on a Bruker AM-400 spectrometer equipped with a previously described home built probehead.[23] The temperature was measured with an accuracy of ±0.5 K after all corrections using a built-in Pt resistor. The $\pi/2$ pulse length

(10) Jenkins, B. G.; Lauffer, R. B. *Inorg. Chem.* **1988**, *27*, 4730.
(11) Peters, J. A. *Inorg. Chem.* **1988**, *27*, 4686.
(12) Bryden, C. C.; Reilley, C. N. *Anal. Chem.* **1982**, *54*, 610.
(13) Spirlet, M. R.; Rebizant, J.; Loncin, M. F.; Desreux, J. F. *Inorg. Chem.* **1984**, *23*, 4278.
(14) Swift, T. J.; Connick, R. E. *J. Chem. Phys.* **1962**, *37*, 307.
(15) Merbach, A. E. *Pure Appl. Chem.* **1987**, *59*, 161.
(16) Cossy, C.; Helm, L.; Merbach, A. E. *Inorg. Chem.* **1988**, *27*, 1973.
(17) Southwood-Jones, R. V.; Earl, W. L.; Newman K. E.; Merbach, A. E. *J. Chem. Phys.* **1980**, *73*, 5909.
(18) Margerum, D. W.; Cayley, G. R.; Weatherburn, D. C.; Pagenkopf, G. K. In *Coordination Chemistry*; Martell, A. E., Ed.; American Chemical Society: Washington, DC, 1978; Vol. 2.
(19) Amman, C.; Meyer, P.; Merbach, A. E. *J. Magn. Reson.* **1982** *46*, 319.
(20) Vold, R. V.; Waugh, J. S.; Klein, M. P.; Phelps, D. E. *J. Chem. Phys.* **1968**, *48*, 3831.
(21) Meiboom, S.; Gill, D. *Rev. Sci. Instrum.* **1958**, *29*, 688.
(22) Hugi, A. D.; Helm, L.; Merbach, A. E. *Helv. Chim. Acta* **1985**, *68*, 508.
(23) Frey, U.; Helm, L.; Merbach, A. E. *High Pressure Res.* **1990**, *2*, 237.

was approximately 15 μs, depending slightly on sample concentration and temperature.

Results

UV–Visible Spectroscopy. A single absorption band for the solutions of $[Eu(DTPA)(H_2O)]^{2-}$ and $[Eu(DOTA)(H_2O)]^{-}$ complexes was observed in the 392 nm < λ < 397 nm range, while in the case of $[Eu(TETA)]^{-}$ the band detected in the same range was split into two peaks at 393.8 and 394.6 nm. The peak intensities (ε) and positions of the maxima (λ) decrease on increasing the temperature from 278 to 358 K. The relative intensities of the two peaks of $[Eu(TETA)]^{-}$ do not change, but this could be the result of the equilibrium of two different species, with negligible enthalpy of reaction. Graeppi[24] measured the $^7F_0$–$^5D_0$ transition of $[Eu(TETA)]^{-}$ in the 578 nm < λ < 581 nm range at different temperatures and observed a single absorption band. This very sensitive transition excludes reliably the formation of different species in our studied temperature range. Taking into account the results published for $[Eu(EDTA)(H_2O)_n]^{-}$, where solvation equilibria between two species was proved,[25] only single species could be detected in the solutions of the complexes we studied.[26]

Variable-Temperature NMR. We measured the temperature dependence of the ^{17}O NMR longitudinal and transverse relaxation rates as well as the chemical shifts of aqueous solutions of $[Gd(DTPA)(H_2O)]^{2-}$, $[Gd(DOTA)(H_2O)]^{-}$, and $[Gd(TETA)]^{-}$. The observed acceleration of the relaxation rates and the observed shift of the resonance frequencies can be described by the formulas developed by Swift and Connick[14] for $1/T_2$ (eq 3) and Δω (eq 4), the chemical shift difference, and by Zimmermann and Brittin[29] for $1/T_1$ (eq 5). As an extension to earlier formulations, we show outer-sphere contributions to relaxation and chemical shift explicitly.

$$\frac{1}{T_2}-\frac{1}{T_{2A}}=\frac{P_m}{T_{2r}}= P_m\left[\frac{1}{\tau_m}\frac{(1/\tau_m+1/T_{2m})/T_{2m}+(\Delta\omega_m)^2}{(1/\tau_m+1/T_{2m})^2+(\Delta\omega_m)^2}+\frac{1}{T_{2os}}\right] \quad (3)$$

$$\omega-\omega_A=P_m\Delta\omega_r= P_m\left[\frac{\Delta\omega_m}{(\tau_m/T_{2m}+1)^2+\tau_m^2(\Delta\omega_m)^2}+\Delta\omega_{os}\right] \quad (4)$$

$$\frac{1}{T_1}-\frac{1}{T_{1A}}=\frac{P_m}{T_{1r}}=P_m\left(\frac{1}{\tau_m+T_{1m}}+\frac{1}{T_{1os}}\right) \quad (5)$$

Symbols without index ($1/T_2$, $1/T_1$, and ω) apply to quantities measured in systems containing the paramagnetic cations. $1/T_{2A}$ and $1/T_{1A}$ are the relaxation rates in acidified water, and $1/T_{2m}$ and $1/T_{1m}$ are those from water directly coordinated to the Gd^{3+} ion. ω_A and ω_m are the ^{17}O NMR chemical shifts from acidified water and from water bound to the paramagnetic cation expressed in rad s^{-1}. $1/T_{2r}$ and $1/T_{1r}$ refer to ^{17}O reduced relaxation rates, and $\Delta\omega_r$ refers to the reduced chemical shift observed for the NMR signal of bulk water caused by the presence of the Gd^{3+} ions. The first term in eq 3 describes the first-coordination-shell effect, and the second term, $1/T_{2os}$, includes the influences of all further coordination shells. $\Delta\omega_{os}$ and $1/T_{1os}$ give the sum of all outer-sphere contributions to $\Delta\omega_r$ and $1/T_{1r}$. P_m is the partial molar fraction of solvent in the first coordination sphere of the cation, and τ_m is the mean lifetime of a water molecule in it.

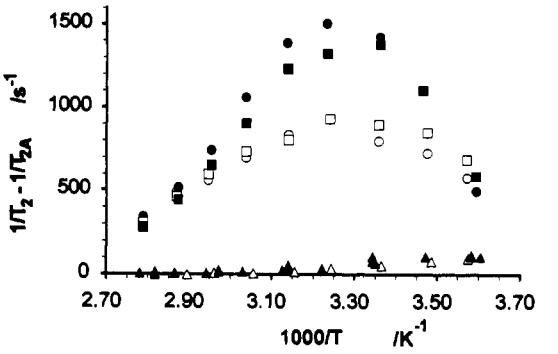

Figure 2. Temperature dependence of ^{17}O NMR transverse relaxation rate increase due to the presence of $[Gd(DTPA)(H_2O)]^{2-}$ (●, ○), $[Gd(DOTA)(H_2O)]^{-}$ (■, □), and $[Gd(TETA)]^{-}$ (▲, △). Filled symbols correspond to 9.4-T and open symbols to 4.7-T results, respectively.

The differences of the transverse relaxation rates measured with and without paramagnetic complexes are shown in Figure 2. The $DTPA^{5-}$ and the $DOTA^{4-}$ complexes, which both contain one water molecule in the first coordination sphere, show typical Swift–Connick temperature behavior, the negative slope at low temperature corresponding to the kinetic region. However for the $TETA^{4-}$ complex we observe only a small increase in the transverse relaxation rate. The phenomenon can be explained in three different ways.

First, a small part of the $TETA^{4-}$ complex may be present as a monoaqua species, leading to a very small value of P_m. We reject this possibility on the basis of our UV–visible spectroscopy measurements. Second, a small amount of octaaqua ion may be present. This supposition was checked by measuring samples at different ligand excess (6–50%) and pH (7.7–8.5). These data (see supplementary material) are close to the values shown in Figure 2, excluding this phenomenon. Finally, it is possible that no water molecule is found in the first coordination sphere of the gadolinium(III) ion in this complex, which means P_m is zero, and the entire increase in relaxation can be attributed to a second-sphere effect.

To be able to describe the temperature dependence of the $1/T_{2r}$ data, we have to know the temperature variations of the different NMR and kinetic parameters. The mean lifetime τ_m is related to the pseudo-first-order rate constant for the exchange of a particular solvent molecule, k_{ex}, whose temperature dependence is given by the Eyring equation (6), where $\Delta S^{\ddagger}$ and $\Delta H^{\ddagger}$ are the activation entropy and the activation enthalpy, respectively.

$$\frac{1}{\tau_m}=k_{ex}=\frac{k_B T}{h}\exp(\Delta S^{\ddagger}/R-\Delta H^{\ddagger}/RT) \quad (6)$$

The temperature dependence of $\Delta\omega_m$, the chemical shift between the bound and the free solvent, has been successfully described by a power series of the inverse temperature.[27] In the present case, however, only the first term due to hyperfine interaction between the unpaired electrons of the Gd^{3+} ion and the ^{17}O nucleus of bound water will be considered (eq 7), where g_L is the Landé

$$\Delta\omega_m=\frac{g_L\mu_B}{\gamma_I}\frac{S(S+1)}{3k_BT}\frac{A}{\hbar}\omega_I \quad (7)$$

factor, μ_B is the Bohr magneton, γ_I is the gyromagnetic ratio of the nucleus I (which is ^{17}O in this case), S is the electron spin quantum number of Gd^{3+} (which is $^7/_2$), and $A/\hbar$ is the hyperfine

(24) Graeppi, N. Personal communication, University of Lausanne.
(25) Geier, G.; Karlen, U.; von Zelewsky, A. *Helv. Chim. Acta* **1969**, *52*, 1967.
(26) For $[Ln(DOTA)(H_2O)]^{-}$ (Ln = Eu, Tb) the low-temperature limiting ^1H and ^{13}C spectra support the presence of two isomeric forms. The structures of the two isomers differ in the layout of the acetate arms, the cyclododecane ring conformation being identical in both species.[27,28]
(27) Brittain, H. G.; Desreux, F. F. *Inorg. Chem.* **1984**, *23*, 4459.
(28) Aime, S.; Botta, M.; Ermondi, G. *Inorg. Chem.* **1992**, *31*, 4291.
(29) Zimmermann, J. R.; Brittin, W. E. *J. Phys. Chem.* **1957**, *61*, 1328.
(30) Bloembergen, N. *J. Chem. Phys.* **1957**, *27*, 595.

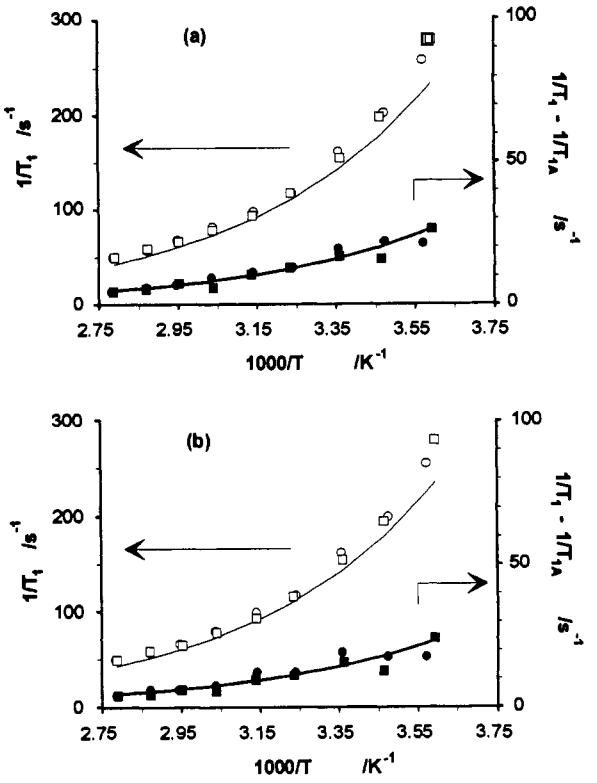

Figure 3. Longitudinal ^{17}O NMR relaxation rates data for (a) 0.05 *m* $[Gd(DTPA)(H_2O)]^{2-}$ and (b) 0.05 *m* $[Gd(DOTA)(H_2O)]^-$ in water as a function of temperature and magnetic field: (□) 9.4 T; (○) 4.7 T. The thin curve shows the relaxation rates, $1/T_{1A}$, of acidified water as a function of temperature. Filled symbols represent the relaxation increase caused by the paramagnetic complex, and the thick curve represents the best fit through these points.

coupling constant. The outer-sphere contribution to the chemical shift is assumed to be linearly related to $\Delta\omega_m$ by a constant C_{os} (eq 8).

$$\Delta\omega_{os} = C_{os}\Delta\omega_m \tag{8}$$

The relaxation of an ^{17}O nucleus in the first coordination sphere of a paramagnetic ion can be expressed as a sum of three relaxation mechanisms: (i) the relaxation due to interaction of the electric quadrupole moment with electric field gradients, (ii) the scalar interaction of the nuclear spin with the electron spin, and (iii) the dipole–dipole interaction of the nuclear spin with the electron spin (eq 9).

$$\frac{1}{T_{jm}} = \frac{1}{T_{jq}} + \frac{1}{T_{jsc}} + \frac{1}{T_{jdd}} \qquad j = 1, 2 \tag{9}$$

In the case of the transverse relaxation, the scalar contribution $1/T_{2sc}$ is by far the most important one,[31] and we neglect therefore the other two (eq 10). In this last equation ω_s is the Lamor

$$\frac{1}{T_{2m}} \cong \frac{1}{T_{2sc}} = \frac{S(S+1)}{3}\left(\frac{A}{\hbar}\right)^2\left(\tau_{s1} + \frac{\tau_{s2}}{1+\omega_s^2\tau_{s2}^2}\right) \tag{10}$$

frequency of the metal electron spin and $1/\tau_{sj}$ is the sum of the exchange rate constant and the electron spin relaxation time (eq 11). The electron spin relaxation rates for metal ions in solution

$$\frac{1}{\tau_{sj}} = \frac{1}{\tau_m} + \frac{1}{T_{je}} \qquad j = 1, 2 \tag{11}$$

with $S \geq 1/2$ are normally governed by a transient zero-field splitting (ZFS), induced by distortions of the complex. Analytical expressions are given by McLachlan[32] in the limit of $\omega_s\tau_v \ll 1$ (eqs 12–14).[33] In these equations Δ^2 is the trace of the square

$$\frac{1}{T_{1e}} = \frac{1}{25}\Delta^2\tau_v[4S(S+1) - 3](J_1 + 4J_2) \tag{12}$$

$$\frac{1}{T_{2e}} = \frac{1}{50}\Delta^2\tau_v[4S(S+1) - 3](J_0 + 5J_1 + 2J_2) \tag{13}$$

$$J_j = [1 + (j\omega_s\tau_v)^2]^{-1} \tag{14}$$

of the zero-field-splitting (ZFS) tensor and τ_v is the correlation time for the modulation of the ZFS. It is generally assumed that the temperature dependence of τ_v follows an Arrhenius behavior (eq 15). The electron spin relaxation times T_{1e} and T_{2e} of the

$$\tau_v = \tau_v^{298}\exp\left[\frac{E_v}{R}\left(\frac{1}{T} - \frac{1}{298}\right)\right] \tag{15}$$

Gd^{3+} ion are generally very long (of the order of 10^{-7}–10^{-9} s) and allow therefore to a very good approximation the use of eq 16 instead of eq 10.

$$\frac{1}{T_{2m}} \cong \frac{1}{T_{2sc}} \cong \frac{S(S+1)}{3}\left(\frac{A}{\hbar}\right)^2\tau_{s1} \tag{16}$$

In the case of the longitudinal relaxation, the important contributions come from the dipolar relaxation $1/T_{1dd}$ and from the quadrupole relaxation $1/T_{1q}$. These relaxation rates are both mostly governed by the correlation time τ_c describing the rotational motion of the whole complex (eqs 17–19). The oxygen–metal

$$\frac{1}{T_{1dd}} = \frac{S(S+1)\gamma_I^2\gamma_S^2\hbar^2}{15r^6}\left(6\tau_{d1} + \frac{14\tau_{d2}}{1+\omega_s^2\tau_{d2}^2}\right) \tag{17}$$

$$\frac{1}{\tau_{dj}} = \frac{1}{T_{je}} + \frac{1}{\tau_m} + \frac{1}{\tau_c} \qquad j = 1, 2 \tag{18}$$

$$\frac{1}{T_{1q}} = \frac{3\pi^2}{10}\frac{2I+3}{I^2(2I-1)}\chi^2\left(1 + \frac{\eta^2}{3}\right)\tau_c \tag{19}$$

distance, r, was fixed to 2.5 Å.[34] The product $\chi(1 + \eta^2/3)^{1/2}$, which contains the quadrupole coupling constant χ and the asymmetry parameter η, was set to the value of pure water, that is 7.58 MHz. The temperature variation of the rotational correlation time, τ_c, can be expressed by eq 20.

$$\tau_c = \tau_c^{298}\exp\left[\frac{E_c}{R}\left(\frac{1}{T} - \frac{1}{298}\right)\right] \tag{20}$$

The temperature dependence of the longitudinal relaxation rates of the $[Gd(DTPA)(H_2O)]^{2-}$ and $[Gd(DOTA)(H_2O)]^-$ solutions and of acidified water are shown in Figure 3. The increase in relaxation due to the interaction with the paramagnetic center represents only a few percent of the total observed relaxation rates and so is attributed only to the inner-sphere effect ($1/T_{1os}$

(31) $1/T_{2q}$ is identical to $1/T_{1q}$ as expressed by eq 19, and $1/T_{2dd}$ is given by

$$\frac{1}{T_{2dd}} = \frac{S(S+1)\gamma_I^2\gamma_S^2\hbar^2}{15r^6}\left(7\tau_{d1} + \frac{13\tau_{d2}}{1+\omega_s^2\tau_{d2}^2}\right)$$

The validity of the approximation was verified by using rotational correlation times as obtained from $1/T_{1r}$; the sum of these two relaxation rates calculated is at most 5% of the scalar relaxation rate; the approximation introduced above (eq 10) is fully justified.

(32) McLachlan, A. D. *Proc. R. Soc. London, A* **1964**, *280*, 271.
(33) Powell, D. H.; Brücher, E.; Gonzalez, G.; Grinberg, O. Y.; Köhler, K.; Lebedev, Y. S.; Merbach, A. E.; Micskei, K.; Ottaviani, F.; von Zelewsky, A. *Helv. Chim. Acta*, in press.
(34) Helm, L.; Merbach, A. E. *Eur. J. Solid State Inorg. Chem.* **1991**, *28*, 245.

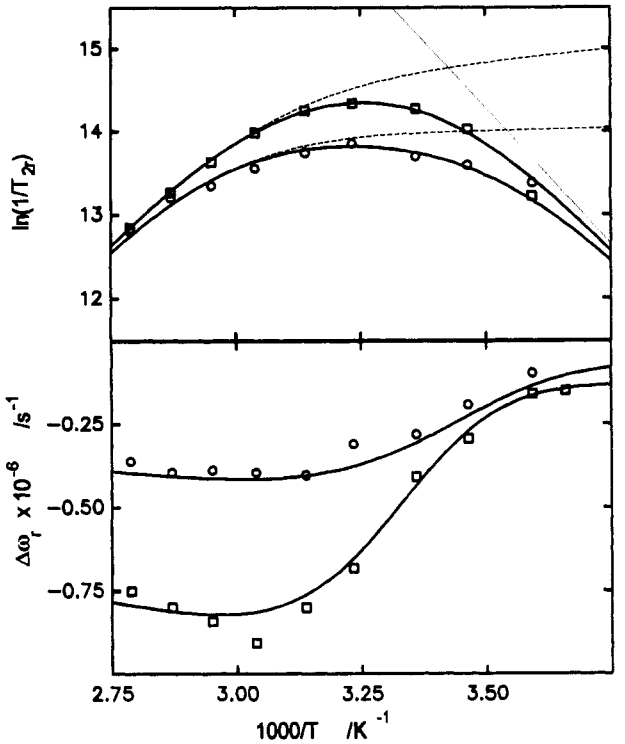

Figure 4. Variable-temperature ^{17}O NMR data for 0.05 *m* [Gd(DTPA)(H_2O)]$^{2-}$ in water showing $\ln(1/T_{2r})$ and $\Delta\omega_r$ vs inverse temperature: (□) 9.4-T data; (○) 4.7-T data. The curves are the result of a simultaneous fit of all data. The short dashed curve shows the contribution of $1/\tau_m$, and the long dashed curves show the contribution of $1/T_{2m}$ to $1/T_{2r}$.

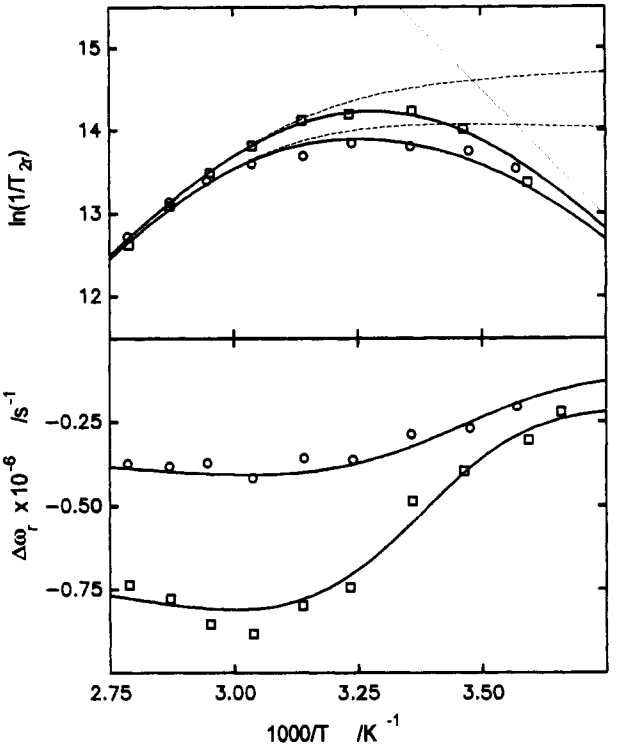

Figure 5. Variable-temperature ^{17}O NMR data for 0.05 *m* [Gd(DOTA)(H_2O)]$^{-}$ in water showing $\ln(1/T_{2r})$ and $\Delta\omega_r$ vs inverse temperature: (□) 9.4-T data; (○) 4.7-T data. The curves are the result of a simultaneous fit of all data. The short dashed curve shows the contribution of $1/\tau_m$, and the long dashed curves show the contribution of $1/T_{2m}$ to $1/T_{2r}$.

= 0). A least-squares fit of these data allows a rough estimation of the rotational correlation times and their activation energies (eqs 5 and 17–20) for DTPA (DOTA): τ_c^{298} = 103 ± 10 ps (90 ± 15 ps) and E_c = 18 ± 2 kJ mol^{-1} (17 ± 3 kJ mol^{-1}).

For the analysis of the transverse relaxation rates and the chemical shifts, a combined nonlinear least-squares treatment of all corresponding data was performed using eqs 3, 4, 6–8, and 11–16.[35] In a first approximation we neglected the contribution from the outer-sphere interaction with the Gd^{3+}. The adjusted parameters are ΔH^*, ΔS^* (or k_{ex}^{298}), $A/\hbar$, C_{OS}, τ_v^{298}, E_v, and Δ^2 ($1/T_{2OS}$ = 0). The last three parameters defining the electronic relaxation rate $1/T_{1e}$ are strongly correlated, leading to relatively large statistical errors. The results are given in Table II, and the calculated curves for DTPA and DOTA are shown in Figures 4 and 5, respectively.

Variable-Pressure NMR. The variable-pressure measurements were performed at 285.6 K/337.4 K (DTPA) and 285.0 K/339.8 K (DOTA) and the results are given in Figure 6. At the lower temperatures $1/T_{2r}$ depends mainly on $k_{ex} = 1/\tau_m$ whereas at the higher ones $1/T_{2m}$ gives the major contribution (see Figures 4 and 5). The pressure dependence of the exchange rate constant k_{ex} is usually assumed to be a quadratic function of the pressure P (eq 21). In this equation $(k_{ex})_0^T$ is the rate constant at zero

$$\ln(k_{ex}) = \ln(k_{ex})_0^T - P\Delta V_0^*/RT + P^2\Delta\beta^*/2RT \quad (21)$$

pressure and temperature T, ΔV_0^* is the activation volume of the reaction at zero pressure, and $\Delta\beta^*$ is the compressibility coefficient of activation.[15] Very often the deviation from linear behavior is well within experimental error, and $\Delta\beta^*$ is therefore set to zero.[36-38]

The evaluation of the pressure dependence of $1/T_{2m}$ is more difficult (eq 16). In earlier studies is was found that the scalar coupling constant $A/\hbar$ is nearly pressure independent.[37] We fixed it therefore to its value at ambient pressure. The pressure dependence of the scalar correlation time τ_{s1} (eq 11) is given by the pressure dependence of the electron spin relaxation rate $1/T_{1e}$ and the pressure dependence of the exchange rate k_{ex}. At the higher temperatures (337.4 and 339.8 K) τ_{s1} is about 30–50% governed by $1/T_{1e}$ and 70–50% by k_{ex}. The results obtained at both temperatures were fitted simultaneously to eqs 3, 11, 16, and 21 with variable parameters ΔV^* and $(k_{ex})_0^T$, and $1/T_{1e}$ was kept pressure independent. $1/T_{1e}$ is related to τ_v according to eq 12, and reasonable pressure variation of τ_v ($|\Delta V_v^*| \leq 5$ cm^3 mol^{-1}) has no effect on the kinetic ΔV^* within the reported experimental uncertainty.

Discussion

The rate of water exchange from the inner sphere of a metal ion is affected strongly by the substitution of one or more water molecules by a coordinated ligand. For the complexes of the first-row transition elements there are a lot of experimental data showing that multidentate ligands increase significantly the rate of exchange of the remaining water molecules.[18] Contrary to these results, the water-exchange rate was found to be lower for the [Gd(PDTA)$(H_2O)_2$]$^-$ complex (k_{ex}^{298} = 3.3 × 10^8 s^{-1}) than

(35) During the fitting procedure, a higher weight was given to relaxation data as compared to chemical shift data; due to relatively small observed shifts (20–120 Hz) compared to observed line widths of 100–500 Hz, the uncertainty in $\Delta\omega_r$ is high.

(36) This approximation was further checked by using $\Delta\beta^*$ as a variable in the fitting procedure, leading to the following values for DTPA (DOTA): ΔV^*/cm^{-3} mol^{-1} = +14.4 ± 0.5 (+12.6 ± 0.3), $10^{-2}\Delta\beta^*$/cm^{-3} mol^{-1} MPa^{-1} = +1.9 ± 0.5 (+2.3 ± 0.3). Using this procedure, the goodness of the fit is not significantly improved and the difference in ΔV^* values is within the error accepted for such determinations (±1 cm^{-3} mol^{-1}, but at least 10%).

(37) Cossy, C.; Helm, L.; Merbach, A. E. *Inorg. Chem.* **1989**, *28*, 2699.

(38) Ducommun, Y.; Newman, K. E.; Merbach, A. E. *Inorg. Chem.* **1980**, *19*, 3696.

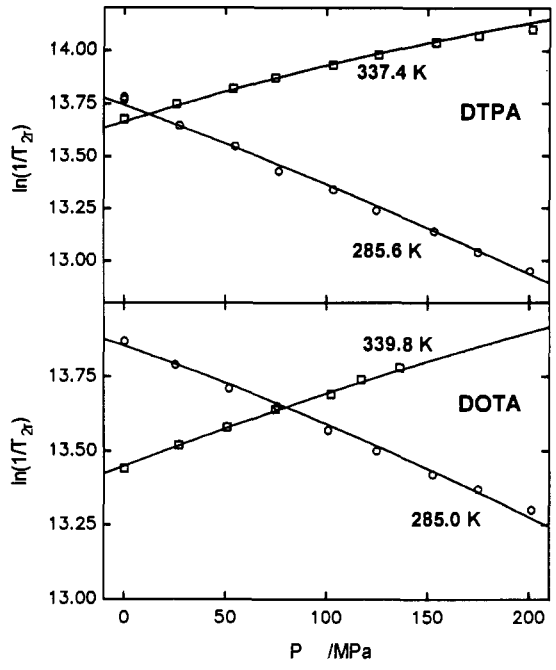

Figure 6. Variable-pressure ^{17}O NMR data for 0.05 *m* [Gd(DTPA)$(H_2O)]^{2-}$ and [Gd(DOTA)$(H_2O)]^-$ in water. The curves represent the result of a simultaneous fit of the data, measured at two temperatures, for DTPA and DOTA, respectively.

for $[Gd(H_2O)_8]^{3+}$ ($k_{ex}^{298} = 1.19 \times 10^9$ s^{-1}).[39] Unfortunately, there are no other data known for the lanthanide complexes, but our results obtained for [Gd(DTPA)$(H_2O)]^{2-}$ and [Gd(DOTA)$(H_2O)]^-$ (Table II) show the same trend, since the water-exchange rates for these complexes are more than 2 orders of magnitude lower than that for $[Gd(H_2O)_8]^{3+}$. As a consequence of the unexpectedly slow water exchange, at lower temperatures the transverse relaxation rate of $H_2{}^{17}O$ is controlled by the chemical exchange (Figure 2.). The explanation of the different behaviors of the complexes of the first-row transition elements and the lanthanides is not easy. We can take into consideration that the chemical bonds in the lanthanide complexes are predominantly ionic, while in the complexes of transition metals, the bonds are partly covalent, and as was discussed by Margerum et al., in the case of the Ni^{2+} complexes[18] the increasing σ-donating strength of the coordinated ligand leads to the increase in the water-exchange rate.[18] The acetate groups are weak σ-donors, and the labilizing effect of the polyacetate ligands is relatively low.[4,18]

For interpretation of the low water-exchange rate of the complexes of $DTPA^{5-}$ and $DOTA^{4-}$, the obtained activation volume data are also useful (Table II). The activation volume for the water exchange of $[Gd(H_2O)_8]^{3+}$ was not determined, but the data obtained for the Tb^{3+}–Tm^{3+} series ($\Delta V^{\ddagger} \approx -6$ cm^3 mol^{-1})[37] clearly indicate a concerted associative I_a mechanism for these elements, which can be assumed to be valid for the next neighbor in the series, the Gd^{3+} aqua ion. However, the activation volumes obtained for the water exchange of [Gd(DTPA)$(H_2O)]^{2-}$ and [Gd(DOTA)$(H_2O)]^-$ are large and positive, indicating a mechanism close to a limiting dissociative (D) mechanism for the water exchange. These activation volumes are the largest values compared with those for other ions: e.g., a value of +7.2 cm^3 mol^{-1} has been reported for $Ni(H_2O)_6^{2+}$.[38] The significant change in the mechanism of the water exchange is probably the result of steric hindrance. In the complex, the Gd^{3+} ion is surrounded

Table II. Kinetic and NMR Parameters Derived from Relaxation and Chemical Shift Data as a Function of Temperature and Pressure

	[Gd(DTPA)$(H_2O)]^{2-}$	[Gd(DOTA)$(H_2O)]^-$
$10^{-6}k_{ex}^{298}$/s^{-1}	4.1 ± 0.3	4.8 ± 0.4
$\Delta H^{\ddagger}$/kJ mol^{-1}	52.0 ± 1.4	48.8 ± 1.6
$\Delta S^{\ddagger}$/J mol^{-1} K^{-1}	+56.2 ± 5	+46.6 ± 6
$\Delta V^{\ddagger}$/cm^3 mol^{-1} [a]	+12.5 ± 0.2	+10.5 ± 0.2
$10^{-6}(A/\hbar)$/rad s^{-1}	−3.8 ± 0.2	−3.4 ± 0.3
C_{os}	0.13 ± 0.06	0.25 ± 0.08
$10^{-19}\Delta^2$/s^{-2}	1.5 ± 0.2	1.2 ± 0.3
$10^{+13}\tau_v^{298}$/s	6.3 ± 0.8	3.8 ± 0.4
E_v/kJ mol^{-1}	7 ± 4	6 ± 4

[a] The fitted exchange rate constants at zero pressure are as follows. DTPA system: $(k_{ex})_0^{285.6} = 1.37 \times 10^6$ s^{-1}, $(k_{ex})_0^{337.4} = 5.70 \times 10^7$ s^{-1}. DOTA system: $(k_{ex})_0^{285.0} = 1.83 \times 10^6$ s^{-1}, $(k_{ex})_0^{339.8} = 6.24 \times 10^7$ s^{-1}.

Table III. Comparison of Relevant ESR Parameters for Different Gd^{3+} Complexes

complex[a]	$10^{-19}\Delta^2$/s^{-2}	$10^{+13}\tau_v^{298}$/s	E_v/kJ mol^{-1}
$[Gd(H_2O)_8]^{3+}$ [b]	9.3	72	15.4
[Gd(PDTA)$(H_2O)_2]^-$ [b]	8.0	480	10.2
[Gd(DTPA-BMA)$(H_2O)]$[b]	3.8	1400	17.6
[Gd(DTPA)$(H_2O)]^{2-}$ [c]	1.5	6.3	7
[Gd(DOTA)$(H_2O)]^-$ [c]	1.2	3.8	6

[a] $PDTA^{4-}$ = 1,3-propylenediaminetetraacetate; $DTPA\text{-}BMA^{3-}$ = diethylenetriaminepentaacetate bis(methylamide). [b] From ref 33. [c] This work.

by the functional groups of $DTPA^{5-}$ or $DOTA^{4-}$ and there is only enough space for the coordination of one water molecule. As a consequence, during the water exchange there is no possibility for the increase of the coordination number to 10. The entering H_2O molecule can be coordinated only on the site of the leaving H_2O and cannot participate in the bond-breaking process, so that the exchange is relatively slow. In the exchange reaction of the Gd^{3+} aqua ion, the species $[Gd(H_2O)_8]^{3+}$ can easily coordinate a ninth H_2O molecule, forming a $[Gd(H_2O)_9]^{3+}$ intermediate, which to a small extent participates in an aquation equilibrium, as shown from neutron-scattering studies on aqueous solutions of Ln^{3+} ions.[34] As a result of this equilibrium, the coordination of the ninth molecule is only weakly hindered. It helps in the bond breaking of the leaving H_2O, and the process can be faster than the dissociation of H_2O from [Gd(DTPA)$(H_2O)]^{2-}$ or [Gd(DOTA)$(H_2O)]^-$ in spite of the somewhat longer Ln^{3+}–OH_2 bonds in the complexes.[40,41] This dissociative activation mode is further supported by the large activation enthalpies $\Delta H^{\ddagger}$ and positive activation entropies $\Delta S^{\ddagger}$ (Table II).

In the discussion of the results obtained for the [Gd(DTPA)$(H_2O)]^{2-}$ and [Gd(DOTA)$(H_2O)]^-$ complexes, we can distinguish between parameters giving information on the electron spin relaxation and kinetic parameters linked to the water exchange from the first coordination sphere. Until now, information on the electron spin relaxation of these complexes has not been available. We can compare our results to ESR and NMR data obtained on the aqua ion and on similar Gd^{3+} complexes. From Table III we see that the trace of the square of the ZFS tensor, Δ^2, is smaller for [Gd(DTPA)$(H_2O)]^{2-}$ and [Gd(DOTA)$(H_2O)]^-$ than for the other systems and the correlation time, τ_v^{298}, for the modulation of the ZFS is much shorter even than in the water complex. The distortion of the ZFS may be caused by impact of the complex with solvent water molecules.[42] In our case, where a relatively large and rigid ligand is bound to the paramagnetic ion, such a process may be less effective.[43] However, the binding of a ligand can lead to an anisotropy of the **g** tensor that can be the source of other relaxation mechanisms

(39) The rate constant 1.06×10^9 s^{-1} for the water exchange of the Gd^{3+} ion was obtained by assuming the presence of $[Gd(H_2O)_9]^{3+}$ ions.[17] The results of neutron diffraction studies proved the predominance of [Gd(DTPA)$(H_2O)]^{3+}$ ions, and the recalculated value of the rate constant is $k_{ex}^{298} = (9/8) \times 1.06 \times 10^9$ s^{-1} $= 1.19 \times 10^9$ s^{-1}.

(40) Stezowsky, J. J.; Howard, J. L. *Isr. J. Chem.* **1984**, *24*, 323.
(41) Sinha, S. P. *Struct. Bonding (Berlin)* **1976**, *25*, 69.
(42) Bloembergen, N.; Morgan, L. O. *J. Chem. Phys.* **1961**, *34*, 842.
(43) Dwek, R. A. *Adv. Mol. Relax. Processes* **1972**, *4*, 1.

for the electron spin, such as spin rotation interaction, so that the values we obtain may not be very accurate.

The exchange of water molecules between the inner sphere of Gd^{3+} and the bulk water is of high importance in MRI, since the paramagnetic effect on bound water is transferred to the bulk water (and to the tissue) by this process. The optimal value of the residence lifetime, τ_m, for obtaining high relaxivities in MRI depends mainly on the rotational correlation time, τ_c, of the complex and on the MRI frequency. In freely rotating complexes, the longitudinal relaxation time of water protons in the bound state, T_{1m}^{proton}, is dominated by the rotational correlation time τ_c and is of the order of 10^{-4}–10^{-6} s. Because $T_{1m}^{proton} \gg \tau_m$, the influence of the proton residence time, for which the water residence time can be taken as an upper limit, on the relaxivity is small in this case. If, however, the complex is immobilized, τ_c becomes longer and can have the same magnitude as T_{1e} and τ_m. According to calculations carried out by Lauffer[4] for such immobilized molecules, the optimal τ_m values are between 10^{-7} and 10^{-8} s at a magnetic field strength of 0.47 T. The residence lifetimes of water molecules as obtained by ^{17}O NMR for $[Gd(DTPA)(H_2O)]^{2-}$ and $[Gd(DOTA)(H_2O)]^{-}$ represent an upper limit for proton residence times and are close to this interval (about 10^{-7} s at 37 °C).

The low oxygen-17 relaxivity observed for $[Gd(TETA)]^{-}$ (Figure 2) is in contrast with its relatively high proton relaxivity[4] (approximately 30–40% of that of $[Gd(DTPA)(H_2O)]^{2-}$ or $[Gd(DOTA)(H_2O)]^{-}$). This finds its explanation in the difference of relaxation mechanisms between proton and oxygen-17. While the latter in the first coordination sphere interacts mainly via scalar interaction with the electron spin of the Gd^{3+} ion, the proton has a much higher contribution from dipole–dipole interaction with the electron spin (about 55 times for the same distance due to the difference in the gyromagnetic ratio). If we consider now a water molecule in the second coordination sphere, where scalar interaction is unimportant, we find a much higher interaction between water protons and the paramagnetic ion than between the oxygen-17 nucleus and the ion.

All these considerations lead to the conclusion that the effectiveness of $[Gd(DTPA)(H_2O)]^{2-}$ and $[Gd(DOTA)(H_2O)]^{-}$ as contrast agents in MRI is limited not by the relatively low water-exchange rates but by T_{1m}, the longitudinal relaxation time of water protons in the first coordination sphere.

Acknowledgment. We thank Prof. J. F. Desreux for providing the TETA ligand used in this study as well as Dr. H. Powell for useful discussions in the interpretation of electron relaxation problems. This work was financially supported by the Swiss National Science Foundation (Grants 20-32703.91 and 70UP-029558) and the Hungarian Scientific Research Foundation (Grants 1643/91 and 1724/91).

Supplementary Material Available: Variable-temperature UV–visible spectra of $[Eu(DTPA)(H_2O)]^{2-}$, $[Eu(DOTA)(H_2O)]^{2-}$, and $[Eu(TETA)]^{2-}$ (Figures S1–S4), variable-temperature ^{17}O relaxation rates of acidified water (Table S1), variable-temperature ^{17}O relaxation rates and chemical shifts of $[Gd(DTPA)(H_2O)]^{2-}$ (Table S2), variable-pressure ^{17}O relaxation rates of $[Gd(DTPA)(H_2O)]^{2-}$ (9.4 T) (Table S3), variable-temperature ^{17}O relaxation rates and chemical shifts of $[Gd(DOTA)(H_2O)]^{-}$ (Table S4), variable-pressure ^{17}O relaxation rates of $[Gd(DOTA)(H_2O)]^{-}$ (9.4 T) (Table S5), and variable-temperature ^{17}O relaxation rates and chemical shifts of $[Gd(TETA)]^{-}$ (Table S6) (9 pages). Ordering information is given on any current masthead page.